Exploring hadron physics in black hole formations: A new promising target of neutrino astronomy

Ken'ichiro Nakazato,[1,*] Kohsuke Sumiyoshi,[2] Hideyuki Suzuki,[3] and Shoichi Yamada[4,†]

[1]*Department of Astronomy, Kyoto University, Kita-shirakawa Oiwake-cho, Sakyo, Kyoto 606-8502, Japan*
[2]*Numazu College of Technology, Ooka 3600, Numazu, Shizuoka 410-8501, Japan*
[3]*Faculty of Science and Technology, Tokyo University of Science, Yamazaki 2641, Noda, Chiba 278-8510, Japan*
[4]*Department of Physics, Waseda University, 3-4-1 Okubo, Shinjuku, Tokyo 169-8555, Japan*

(Received 11 March 2009; revised manuscript received 25 October 2009; published 19 April 2010)

The detection of neutrinos from massive stellar collapses can teach us a great deal not only about source objects but also about microphysics working deep inside them. In this study we discuss quantitatively the possibility to extract information on the properties of dense and hot hadronic matter from neutrino signals coming out of black-hole-forming collapses of nonrotational massive stars. Based on our detailed numerical simulations we evaluate the event numbers for SuperKamiokande, with neutrino oscillations fully taken into account. We demonstrate that the event numbers from a Galactic event are large enough not only to detect but also to distinguish one hadronic equation of state from another by our statistical method, assuming the same progenitor model and nonrotation. This means that the massive stellar collapse can be a unique probe into hadron physics and will be a promising target of the nascent neutrino astronomy.

DOI: 10.1103/PhysRevD.81.083009 PACS numbers: 26.50.+x, 21.65.Mn, 95.85.Ry, 97.60.−s

I. INTRODUCTION

One of the important roles of astrophysics is to explore physics under extreme conditions that are difficult to realize in terrestrial experiments. In this sense, hadron physics at supranuclear densities and nonzero temperatures (e.g., hyperon appearance, quark deconfinement, and so on) is a natural target of astrophysics, and the gravitational collapse of massive stars at the end of their lives will set the stage [1,2]. In particular, black-hole-forming collapses expected for very massive stars, larger than ~30 solar masses ($M_\odot$), will be the most promising sites. Although such an event has not been observed yet, a black hole candidate with an estimated mass of 24–33$M_\odot$ was discovered [3], and this might be a remnant of the collapse of such a massive star. Recently, a regular monitoring of $\sim 10^6$ supergiants within a distance of 10 Mpc was proposed to detect their silent disappearances [4], and the black-hole-forming collapse, which would be invisible optically, might be observed that way.

In our previous studies [5–7], we showed that the event, which we refer to as the ''failed supernova'' hereafter, is as bright in neutrino emissions as ordinary core-collapse supernovae. We also showed that its time evolutions of luminosities and spectra are qualitatively different from those of the ordinary supernova explosion and the ensuing proto-neutron star cooling [8], which may lead to the delayed black hole formation [9,10]. Our numerical data were adopted as a reliable basis to predict the relic neutrino background from stellar collapses [11]. More importantly, however, we also demonstrated, by employing different hadronic equations of state (EOS), that the duration of neutrino emissions from the failed supernova is sensitive to the stiffness of EOS at supranuclear densities and, therefore, that the observation of neutrinos from such an event will provide us with valuable information on the properties of dense and hot hadronic matter as well as on the maximum mass of proto-neutron stars.

Although this approach is simple and robust, and valid irrespective of neutrino oscillations, it cannot distinguish EOS's with a similar duration of neutrino emissions: a soft nucleonic EOS and a hyperonic EOS, for example. In this study, we attempt to break this degeneracy by analyzing in more detail the time variation of neutrino numbers observed at a terrestrial detector, which we refer to as the ''light curve'' hereafter. While we have studied the detection of failed supernova neutrinos, fully taking into account the neutrino oscillation and its parameter dependence so far [12], we innovate a new method here by employing the Kolmogolov-Smirnov (KS) test, which is free from the ambiguity of the distance to the progenitor. We adopt the results of our detailed numerical simulations and evaluate the neutrino event number for SuperKamiokande (SK) as a representative of currently operating neutrino detectors. This is the first serious self-contained attempt to demonstrate that, for Galactic events, it is indeed possible to break the degeneracy for hadronic EOS's by statistical analysis.

We arrange this paper as follows. A brief review of neutrino detection and a description of the newly proposed statistical method are given in Sec. II. The main results of our study are reported in Sec. III. In Sec. IV, we mention

*nakazato@kusastro.kyoto-u.ac.jp
†Also at Advanced Research Institute for Science and Engineering, Waseda University, 3-4-1 Okubo, Shinjuku, Tokyo 169-8555, Japan.

the possible uncertainties and observational issues. Section V is devoted to a summary.

II. METHODS

A. Setups for failed supernova neutrino detection

The evaluation of the light curve of neutrinos from failed supernovae can be roughly divided into three steps. The first step is the computation of the neutrino luminosity and spectrum at the source. The general relativistic ν-radiation-hydrodynamics code, which solves the Boltzmann equations for neutrinos together with the Lagrangian hydrodynamics under spherical symmetry, is utilized to quantitatively compute the dynamics as well as the neutrino luminosities and spectra up to the black hole formation. This code passed a couple of well-known standard tests and a detailed comparison with other simulations [13–15]. The numerical errors are estimated to be $\sim$10% from the computations with lower resolutions in Ref. [16]. The progenitor model with $40M_{\odot}$ [17] is adopted as the initial condition for the dynamical simulations.

A hadronic EOS is needed at this stage. It should be emphasized that it is not our intention in this paper to endorse a particular EOS. However, note that EOS's which are available for astrophysical numerical simulations, that is, subroutines or tables that provide thermodynamic variables in wide ranges of density, temperature, and proton fraction, are very limited at present. For example, an EOS table including hyperons has been provided only by Ishizuka *et al.* [18] so far, based on the relativistic mean field theory. The EOS's by Lattimer and Swesty [19] and by Shen *et al.* [20,21] are the ones from the limited options for the nucleonic EOS. The former is an extension of the compressible liquid drop model with three choices of incompressibility ($K = 180$, 220, 375 MeV) and the latter is based on the same framework as in Ref. [18] but without hyperons. In this paper, we employ the EOS's from Ref. [18] (Hyperon-EOS), Refs. [20,21] (Shen-EOS), and Ref. [19], with $K = 180$ MeV (LS180-EOS) and 220 MeV (LS220-EOS). Whereas the results for the Hyperon-EOS, Shen-EOS, and LS180-EOS have also already been given in Ref. [1], the LS220-EOS model is newly computed.

In Fig. 1, we show the luminosities and average energies of electron-type antineutrinos for these EOS's. The result for the Hyperon-EOS is almost the same as that for the Shen-EOS until hyperons appear around $\sim$0.5 sec, since the two EOS's are identical in the low density regime. The Shen-EOS, which is the stiffest ($K = 281$ MeV) among these EOS's, is sufficiently distinguishable from the other three just by its longer duration (1.345 sec) of neutrino emissions. This will not be the case, on the other hand, for the Hyperon-EOS and the LS-EOS's with $K \sim 200$ MeV because the duration for the Hyperon-EOS (0.682 sec) is not very different from those for the LS180-EOS (0.566 sec) and LS220-EOS (0.784 sec). This is the degeneracy problem mentioned earlier. It is the main purpose of

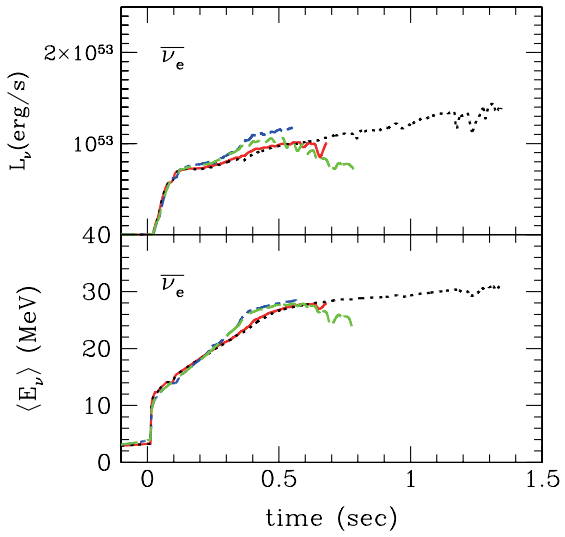

FIG. 1 (color online). Luminosities and average energies of $\bar{\nu}_e$ for four different EOS's, LS180-EOS (dash-dotted line), LS220-EOS (dashed line), Shen-EOS (dotted line), and Hyperon-EOS (solid line). Time is measured from the bounce.

the study to demonstrate that the relatively small difference displayed in Fig. 1 is still sufficient to distinguish one EOS from the others by the statistical analysis given below.

The second step for the evaluation of the light curve is to incorporate the neutrino oscillations, which take place as the Mikheyev-Smirnov-Wolfenstein (MSW) effect during the propagations through the stellar envelope and the Earth. Since the reactions at the detector depend on the neutrino flavor, a proper treatment of the neutrino oscillations is mandatory. In this paper, we ignore the Earth effect, since the event number will not be affected very much [12]. As for the undetermined parameters in the neutrino oscillation, namely, the mixing angle, θ_{13}, and the mass hierarchy, we choose two limiting cases: the normal mass hierarchy with $\sin^2\theta_{13} = 10^{-8}$ and the inverted mass hierarchy with $\sin^2\theta_{13} = 10^{-2}$. For the detailed dependences on the choice of these parameters, we refer readers to Ref. [12].

The last part of the procedure is an evaluation of event numbers at the detector. In this paper, we take SK from currently operating neutrino detectors. The neutrino reactions in the detector that we take into account are as follows:

$$\bar{\nu}_e + p \rightarrow e^+ + n, \tag{1}$$

$$\nu + e \rightarrow \nu + e, \tag{2}$$

$$\nu_e + {}^{16}\mathrm{O} \rightarrow e + {}^{16}\mathrm{F}, \tag{3}$$

$$\bar{\nu}_e + {}^{16}\mathrm{O} \rightarrow e^+ + {}^{16}\mathrm{N}. \tag{4}$$

The first reaction gives a dominant contribution to the

event number and we take its cross section from Ref. [22]. The second reaction occurs for all flavors of neutrino but with different cross sections, which are taken from Ref. [23]. The cross sections for the others are adopted from Ref. [24]. We assume that the fiducial volume is 22.5 kton, and the trigger efficiency is 100% at 4.5 MeV and 0% at 2.9 MeV, which are the values at the end of SuperKamiokande I [25]. The energy resolution was 14.2% for $E_e = 10$ MeV at that time [25] and roughly proportional to $\sqrt{E_e}$ [26], where E_e is the kinetic energy of scattered electrons and positrons. We choose the width of the energy bin to be 1 MeV in this study. The event numbers for the progenitor at a distance of 10 kpc are listed in Table I for eight different combinations of EOS and mixing parameters.

B. Statistical analysis

In order to see if two different hadronic EOS's can be distinguished by the neutrino observations, we take the following strategy. We first generate the "observational data" by Monte Carlo (MC) simulations based on the light curve obtained above for one EOS. We then take the light curve for another EOS as the "theoretical" model and employ the KS test to judge if the difference is statistically significant. In this study, we adopt the Hyperon-EOS for the former and LS180- and LS220-EOS's for the latter.

In our analysis, we utilize the normalized time profiles of the cumulative event numbers for the first 0.5 sec of detections so that we can ignore the neutrino emissions after the black hole formation and the uncertainties of the distance measurement to the progenitor. In this study, we consider two cases, in which the total event numbers up to 0.5 sec, $N_{0.5\ \mathrm{s}}$, are 10 000 and 400. The former roughly corresponds to the source located at the Galactic center while the latter represents an event in the Large Magellanic Cloud (LMC) or Small Magellanic Cloud (SMC).

In the KS test, the so-called KS measure D_{KS} is defined as the maximum difference [27] between the two data:

$$D_{\mathrm{KS}} = \max_{t \le 0.5\ \mathrm{s}} |f_{\mathrm{theor}}(t) - f_{\mathrm{obs}}(t)|, \qquad (5)$$

TABLE I. Event numbers for the progenitor at a distance of 10 kpc. $N_{\mathrm{all}}^{10\ \mathrm{kpc}}$ and $N_{0.5\ \mathrm{s}}^{10\ \mathrm{kpc}}$ denote the event numbers until the end of the simulation and up to 0.5 sec after the bounce, respectively.

EOS	Mixing parameter	$N_{\mathrm{all}}^{10\ \mathrm{kpc}}$	$N_{0.5\ \mathrm{s}}^{10\ \mathrm{kpc}}$
LS180	Normal and $\sin^2\theta_{13} = 10^{-8}$	16 086	12 543
LS220	Normal and $\sin^2\theta_{13} = 10^{-8}$	25 978	11 970
Hyperon	Normal and $\sin^2\theta_{13} = 10^{-8}$	16 490	10 120
Shen	Normal and $\sin^2\theta_{13} = 10^{-8}$	49 513	9745
LS180	Inverted and $\sin^2\theta_{13} = 10^{-2}$	12 136	9169
LS220	Inverted and $\sin^2\theta_{13} = 10^{-2}$	23 656	8820
Hyperon	Inverted and $\sin^2\theta_{13} = 10^{-2}$	9952	6579
Shen	Inverted and $\sin^2\theta_{13} = 10^{-2}$	30 992	6208

where $f_{\mathrm{theor}}(t)$ and $f_{\mathrm{obs}}(t)$ are the theoretical and observational time profiles of neutrino events, respectively. As mentioned already, they are normalized as $f_{\mathrm{theor}}(0.5\ \mathrm{s}) = f_{\mathrm{obs}}(0.5\ \mathrm{s}) = 1$ in our analysis. If $D_{\mathrm{KS}} > 0.016\,22$ (0.0811) for $N_{0.5\ \mathrm{s}} = 10\,000$ (400), the theoretical model is rejected at a confidence level of 99%.

We also employ time-shifted observational data, since we cannot know the onset of neutrino detections precisely. In this case, the KS measure becomes a function of the time shift t_{shift} as

$$D_{\mathrm{KS}}(t_{\mathrm{shift}}) = \max_{t \le 0.5\ \mathrm{s}} |f_{\mathrm{theor}}(t) - f_{\mathrm{obs}}(t - t_{\mathrm{shift}})|, \qquad (6)$$

where the time profiles are normalized as $f_{\mathrm{theor}}(0.5\ \mathrm{s}) = f_{\mathrm{obs}}(0.5\ \mathrm{s} - t_{\mathrm{shift}}) = 1$. If the minimum value of the KS measure with respect to the time shift satisfies the above criteria, i.e., $\min_{t_{\mathrm{shift}}} D_{\mathrm{KS}}(t_{\mathrm{shift}}) > 0.016\,22$ (0.0811) for $N_{0.5\ \mathrm{s}} = 10\,000$ (400), we can conclude at 99% C.L. that the two data are distinct from each other.

III. RESULTS

A. Analysis without time shift

We first show the results of the analysis without the time shift. In Fig. 2, we compare the unnormalized time profiles of cumulative event numbers between MC data ("observational data") randomly picked up from 100 000 realizations for the Hyperon-EOS and the "theoretical"

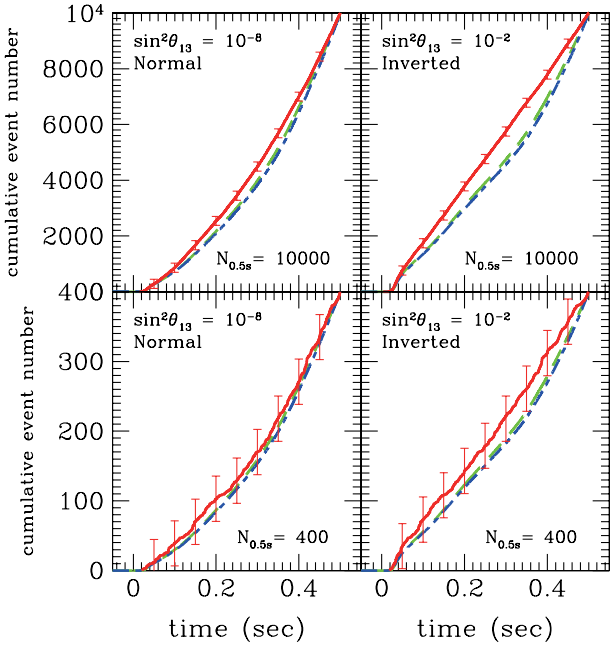

FIG. 2 (color online). Unnormalized time profiles of cumulative event numbers for two mixing parameter sets and two total event numbers. The observational data are shown by solid lines, whereas the theoretical estimations are displayed by dash-dotted lines for the LS180-EOS and dashed lines for the LS220-EOS. The error bars correspond to 99% C.L. in the KS test.

estimations for the LS180-EOS and LS220-EOS. Since the growth rates of neutrino luminosity and mean energy are larger for LS-EOS's than for the Hyperon-EOS (see Fig. 1), the lines for the former are lower than for the latter. The vertical bars correspond to $\pm 0.016\,22$ (0.0811) in the normalized profiles for $N_{0.5\ \mathrm{s}} = 10\,000$ (400), and the theoretical models outside these error bars are rejected by the KS test at 99% C.L. It is clear from the figure that for $N_{0.5\ \mathrm{s}} = 10\,000$ or the Galactic source, we can easily distinguish the Hyperon-EOS from LS-EOS's. In fact, this is true not only for these particular data but also for all 100 000 MC realizations in each set of mixing parameters. Thus we can conclude that the Hyperon-EOS and LS-EOS's employed in this study are distinguishable for Galactic events.

The claim depends on the mixing parameters for events in the LMC or SMC, that is, for $N_{0.5\ \mathrm{s}} = 400$ as can be inferred from Fig. 2. In fact, for the normal mass hierarchy with $\sin^2\theta_{13} = 10^{-8}$, the Hyperon-EOS is not distinguishable from the LS220-EOS (LS180-EOS) for more than 65% (40%) of 100 000 MC realizations. In the case of the inverted mass hierarchy with $\sin^2\theta_{13} = 10^{-2}$, however, the distinction fails 5218 (512) times among 100 000 MC realizations for the LS220-EOS (LS180-EOS). The reason why the latter case of mixing parameters is easier is as follows. The EOS dependence is stronger for muon-type and tau-type neutrinos and their antineutrinos than for their electron-type counterparts (see Fig. 3 of Ref. [1]). A portion of $\bar{\nu}_\mu$ and $\bar{\nu}_\tau$ is converted to $\bar{\nu}_e$, the dominant contributor to the event number via reaction (1). While 16% of $\bar{\nu}_\mu$ and $\bar{\nu}_\tau$ become $\bar{\nu}_e$ for the normal mass hierarchy with $\sin^2\theta_{13} = 10^{-8}$, half of $\bar{\nu}_\mu$ and $\bar{\nu}_\tau$ are converted to $\bar{\nu}_e$ for the inverted mass hierarchy with $\sin^2\theta_{13} = 10^{-2}$, thus yielding the observed EOS dependence of the event numbers.

B. Analysis with time shift

Next, we demonstrate that the conclusion is unchanged if the time shift is included in the analysis. In Fig. 3, the distributions of the KS measures for 100 000 MC realizations are shown as a function of the time shift t_{shift}. The LS180-EOS (LS220-EOS) is employed to obtain the "theoretical" model in the left (right) panel. For Galactic sources, that is, in the case of $N_{0.5\ \mathrm{s}} = 10\,000$, all 100 000 MC realizations have D_{KS} larger than 0.016 22, the lower limit for the rejection by the KS test, for any value of the time shift in the case of the normal mass hierarchy with $\sin^2\theta_{13} = 10^{-8}$. This is all the more true for the inverted mass hierarchy with $\sin^2\theta_{13} = 10^{-2}$.

For $N_{0.5\ \mathrm{s}} = 400$, however, the above conclusion is somewhat compromised. In the case of the normal mass hierarchy with $\sin^2\theta_{13} = 10^{-8}$, for example, the Hyperon-EOS and the LS180-EOS are not distinguishable in more than 90% of 100 000 MC realizations when $t_{\mathrm{shift}} = 0.06$ sec is assumed. For the inverted mass hierarchy with $\sin^2\theta_{13} = 10^{-2}$, on the other hand, more than 75% (90%) of MC realizations have a KS measure larger than the critical value for the LS220-EOS (LS180-EOS). In conclusion, for an event in the LMC or SMC, the success-

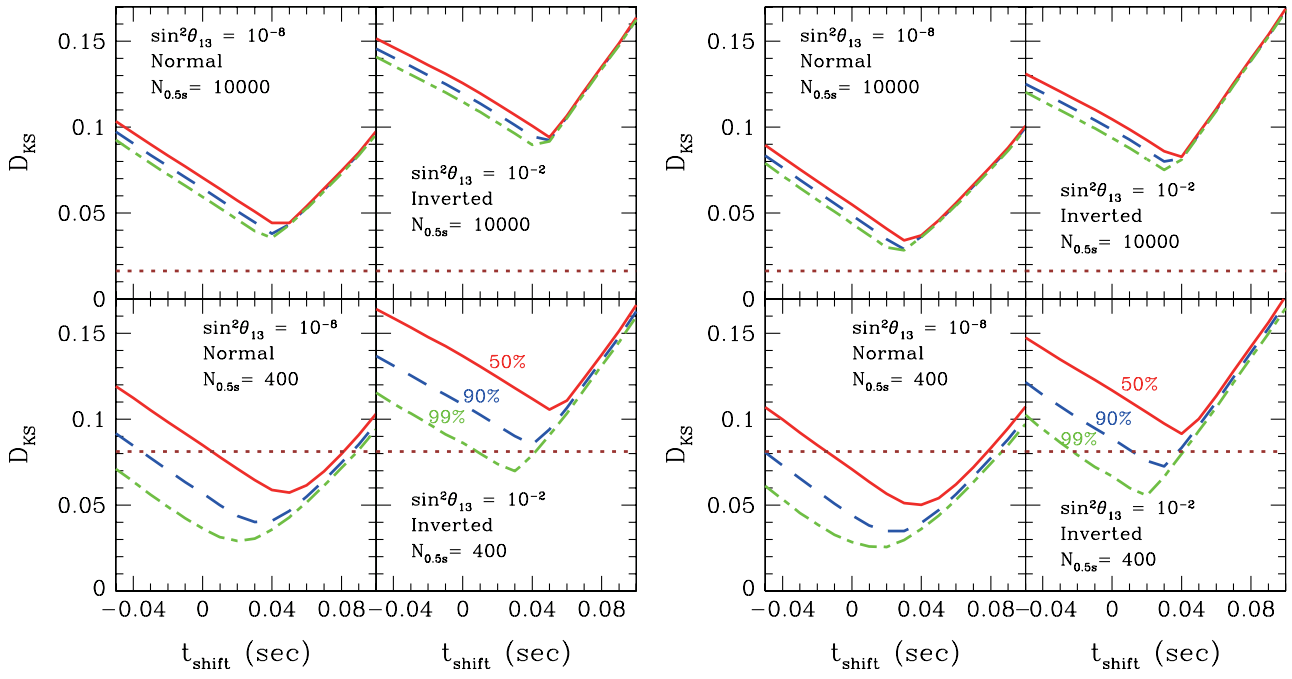

FIG. 3 (color online). The KS measures D_{KS} as a function of the time shift t_{shift} for the LS180-EOS (left panel) and the LS220-EOS (right panel). Respectively, 50%, 90%, and 99% of D_{KS}'s lie above the solid, dashed, and dot-dashed lines in 100 000 MC realizations. The horizontal dotted lines represent the lower limit to reject the model by the KS test.

ful distinction of Hyperon- and LS-EOS's depends on the neutrino mixing parameters; the inverted mass hierarchy with $\sin^2\theta_{13} = 10^{-2}$ is more advantageous.

IV. DISCUSSION

Certainly, there are some issues that remain unaddressed. First of all, investigating other EOS's constructed by different methods is important for future work. In particular, hyperon mixing in neutron star matter has been studied by the microscopic approach [28–30] and this method is desired to be applied to EOS tables including finite temperature. If neutrinos have masses of ~eV, the arrival time depends on the neutrino energy, and the difference becomes ~0.01 sec between the neutrinos with an energy of $E \sim 10$ MeV and those with $\gtrsim 30$ MeV [31] for Galactic sources. Recently, the core-collapse simulations for the same progenitor model were done utilizing a spherically symmetric ν-radiation-hydrodynamics code by another group [32]. While they conclude that their results are in qualitative agreement with our study, there are some quantitative differences. For instance, in the case with the LS180-EOS, they found that the interval time between the bounce and the black hole formation is 0.436 sec, which is ~20% shorter than our result. Further numerical investigation is important.

Multidimensional hydrodynamical effects such as rotations and magnetic fields, which are not taken into account in our model, may also affect the signals. In the context of supernovae explosions, Ref. [33] compared the neutrino signal by a one-dimensional simulation with those by two-dimensional simulations (with and without rotation) for the collapse of a $15M_\odot$ star, adopting the LS180-EOS (see Figs. 1 and 14 of that paper). According to that paper, when the initial rotation of the progenitor core is a constant angular frequency of 0.5 rad s^{-1}, the stellar rotation does not affect the luminosity or mean energy of the emitted neutrinos very much. Incidentally, the neutrino emission after the collapse to a black hole is estimated to be negligible for low-angular momentum cases [34].

Uncertainties with progenitor structures are another concern. While a certain class of progenitors provides similarly short neutrino bursts, it has been shown that the density profile of the outer layer may affect the duration [7]. In particular, if the matter density outside the core is lower, the interval time between the bounce and the black hole formation becomes longer (e.g., 1.477 sec [32] even for the model with $40M_\odot$ [35] and the LS180-EOS). However, if a neutrino event is actually detected, we will be able to determine the direction of the progenitor to some extent by the neutrino detection itself [36], and the progenitor is highly likely to be identified or at least constrained by earlier records of optical observations, as in the case of SN1987A. Then we can study the progenitor dependence much more efficiently.

As discussed in Refs. [4,12], the event rate of the black-hole-forming failed supernovae is estimated to be somewhat low, ~0.008/yr. This problem may be circumvented, however, by deploying a large detector such as Deep-TITAND with a fiducial volume of 5 Mton [37] currently proposed. With this large facility, the event rate goes up to ~0.02/yr since we should be able to detect ~400 neutrinos for the first 0.5 sec of a failed supernova in galaxies as far away as the Andromeda galaxy (M31) at 780 kpc from us. This is large enough to distinguish the EOS's we studied in this paper for the inverted mass hierarchy with $\sin^2\theta_{13} = 10^{-2}$. Note that the cumulative core-collapse supernova rate within this range is 10% of that within 10 Mpc [38], where a regular monitoring of $\sim 10^6$ supergiants is proposed in Ref. [4].

V. SUMMARY

This study is the first serious self-contained attempt to assess the neutrino signals from black-hole-forming failed supernovae, which would be observed by the currently operating terrestrial detector. Based on our detailed numerical simulations, we have evaluated the event number of neutrinos emitted from black-hole-forming failed supernova for some EOS's of nuclear matter. Ambiguities on the neutrino mixing parameters and the onset of the neutrino emission have also been taken into account for the evaluation. Assuming the same progenitor model and nonrotation, we have shown that we will be able to constrain the EOS of nuclear matter not only from the duration time of neutrino emission but also from the time variations of the neutrino event number for the progenitor in our Galaxy. Moreover, in the case of the inverted mass hierarchy with $\sin^2\theta_{13} = 10^{-2}$, the constraint is favorable even for the progenitor in the LMC or SMC. The positive results presented here clearly indicate the importance of further investigations of the hadronic EOS at supranuclear densities based on better formulations, and encourage, in particular, those engaged in the study of the EOS of hadronic matter to prepare their latest results in a form available for astrophysical simulations. We hope this paper will advance such collaborations further.

ACKNOWLEDGMENTS

We are grateful to Akira Ohnishi and Chikako Ishizuka for fruitful discussions. In this work, numerical computations were partially performed on the supercomputers at Research Center for Nuclear Physics (RCNP) at Osaka University, Center for Computational Astrophysics (CfCA) at the National Astronomical Observatory of Japan (NAOJ), Yukawa Institute for Theoretical Physics (YITP) at Kyoto University, Japan Atomic Energy Agency (JAEA), and High Energy Accelerator Research Organization (KEK). This work was partially supported by the Japan Society for Promotion of Science (JSPS)

through Grant No. 18-510 and No. 21-1189, and Grants-in-Aid for scientific research from the Ministry of Education, Culture, Sports, Science and Technology (MEXT) of Japan through Grant No. 17540267, No. 18540291, No. 18540295, No. 19104006, No. 19540252, No. 20105004, and No. 21540281.

[1] K. Sumiyoshi, C. Ishizuka, A. Ohnishi, S. Yamada, and H. Suzuki, Astrophys. J. **690**, L43 (2009).
[2] K. Nakazato, K. Sumiyoshi, and S. Yamada, Phys. Rev. D **77**, 103006 (2008).
[3] A. H. Prestwich *et al.*, Astrophys. J. **669**, L21 (2007).
[4] C. S. Kochanek *et al.*, Astrophys. J. **684**, 1336 (2008).
[5] K. Sumiyoshi, S. Yamada, H. Suzuki, and S. Chiba, Phys. Rev. Lett. **97**, 091101 (2006).
[6] K. Sumiyoshi, S. Yamada, and H. Suzuki, Astrophys. J. **667**, 382 (2007).
[7] K. Sumiyoshi, S. Yamada, and H. Suzuki, Astrophys. J. **688**, 1176 (2008).
[8] T. Totani, K. Sato, H. E. Dalhed, and J. R. Wilson, Astrophys. J. **496**, 216 (1998).
[9] T. W. Baumgarte, H.-Th. Janka, W. Keil, S. L. Shapiro, and S. A. Teukolsky, Astrophys. J. **468**, 823 (1996).
[10] J. A. Pons, A. W. Steiner, M. Prakash, and J. M. Lattimer, Phys. Rev. Lett. **86**, 5223 (2001).
[11] C. Lunardini, Phys. Rev. Lett. **102**, 231101 (2009).
[12] K. Nakazato, K. Sumiyoshi, H. Suzuki, and S. Yamada, Phys. Rev. D **78**, 083014 (2008); **79**, 069901(E) (2009).
[13] S. Yamada, Astrophys. J. **475**, 720 (1997).
[14] S. Yamada, H.-Th Janka, and H. Suzuki, Astron. Astrophys. **344**, 533 (1999).
[15] K. Sumiyoshi *et al.*, Astrophys. J. **629**, 922 (2005).
[16] K. Nakazato, K. Sumiyoshi, and S. Yamada, Astrophys. J. **666**, 1140 (2007).
[17] S. E. Woosley and T. Weaver, Astrophys. J. Suppl. Ser. **101**, 181 (1995).
[18] C. Ishizuka, A. Ohnishi, K. Tsubakihara, K. Sumiyoshi, and S. Yamada, J. Phys. G **35**, 085201 (2008).
[19] J. M. Lattimer and F. D. Swesty, Nucl. Phys. **A535**, 331 (1991).
[20] H. Shen, H. Toki, K. Oyamatsu, and K. Sumiyoshi, Nucl. Phys. **A637**, 435 (1998).
[21] H. Shen, H. Toki, K. Oyamatsu, and K. Sumiyoshi, Prog. Theor. Phys. **100**, 1013 (1998).
[22] A. Strumia and F. Vissani, Phys. Lett. B **564**, 42 (2003).
[23] Y. Totsuka, Rep. Prog. Phys. **55**, 377 (1992).
[24] W. C. Haxton, Phys. Rev. D **36**, 2283 (1987).
[25] J. Hosaka *et al.*, Phys. Rev. D **73**, 112001 (2006).
[26] C. Lunardini and A. Y. Smirnov, Nucl. Phys. **B616**, 307 (2001).
[27] M. G. Kendall and A. Stuart, *The Advanced Theory of Statistics* (Griffin, London, 1979).
[28] M. Baldo, G. F. Burgio, and H.-J. Schulze, Phys. Rev. C **61**, 055801 (2000).
[29] S. Nishizaki, Y. Yamamoto, and T. Takatsuka, Prog. Theor. Phys. **108**, 703 (2002).
[30] H.-J. Schulze, A. Polls, A. Ramos, and I. Vidaña, Phys. Rev. C **73**, 058801 (2006).
[31] J. F. Beacom, R. N. Boyd, and A. Mezzacappa, Phys. Rev. D **63**, 073011 (2001).
[32] T. Fischer, S. C. Whitehouse, A. Mezzacappa, F.-K. Thielemann, and M. Liebendörfer, Astron. Astrophys. **499**, 1 (2009).
[33] A. Marek, and H.-Th. Janka, Astrophys. J. **694**, 664 (2009).
[34] C. L. Fryer, Astrophys. J. **699**, 409 (2009).
[35] S. E. Woosley, A. Heger, and T. Weaver, Rev. Mod. Phys. **74**, 1015 (2002).
[36] S. Ando and K. Sato, Prog. Theor. Phys. **107**, 957 (2002).
[37] M. D. Kistler, H. Yüksel, S. Ando, J. F. Beacom, and Y. Suzuki, arXiv:0810.1959.
[38] S. Ando, J. F. Beacom, and H. Yüksel, Phys. Rev. Lett. **95**, 171101 (2005).